Postprint of: Science of The Total Environment (760): 143408 (2021)

Root-mediated bacterial accessibility and cometabolism of pyrene in soil

Carmen Fernández-López[1], Rosa Posada-Baquero[2], José Luis García[2], José Carlos Castilla-Alcantara[2], Manuel Cantos[2] and Jose Julio Ortega-Calvo[2]

[1]*University Centre of Defense at the Spanish Air Force Academy, Santiago de la Ribera, Spain*
[2]*Instituto de Recursos Naturales y Agrobiología de Sevilla (IRNAS-CSIC), Seville, Spain.*

Keywords: Biodegradation, Polycyclic aromatic hydrocarbons, Bioremediation, Sunflower, Bacteria

*Corresponding author tel: (+34) 95-4624711; fax: (+34) 95-4624002; e-mail: jjortega@irnase.csic.es

Abstract

Partial transformation of pollutants and mobilization of the produced metabolites may contribute significantly to the risks resulting from biological treatment of soils polluted by hydrophobic chemicals such as polycyclic aromatic hydrocarbons (PAHs). Pyrene, a four-ringed PAH, was selected here as a model pollutant to study the effects of sunflower plants on the bacterial accessibility and cometabolism of this pollutant when located at a spatially distant source within soil. We compared the transformation of passively dosed ^{14}C-labeled pyrene in soil slurries and planted pots that were inoculated with the bacterium *Pseudomonas putida* G7. This bacterium combines flagellar cell motility with the ability to cometabolically transform pyrene. Cometabolism of this PAH occurred immediately in the inoculated and shaken soil slurries, where the bacteria had full access to the passive dosing devices (silicone O-rings). Root exudates did not enhance the survival of *P. putida* G7 cells in soil slurries, but doubled their transport in column tests. In greenhouse-incubated soil pots with the same pyrene sources instead located centimeters from the soil surface, the inoculated bacteria transformed ^{14}C-labeled pyrene only when the pots were planted with sunflowers. Bacterial inoculation caused mobilization of ^{14}C-labeled pyrene metabolites into the leachates of the planted pots at concentrations of approximately 1 mg L^{-1}, ten times greater than the water solubility of the parent compound. This mobilization resulted in a doubled specific root uptake rate of ^{14}C-labeled pyrene equivalents and a significantly decreased root-to-fruit transfer rate. Our results show that the plants facilitated bacterial access to the distant pollutant source, possibly by increasing bacterial dispersal in the soil; this increased bacterial access was associated with cometabolism, which contributed to the risks of biodegradation.

GRAPHICAL ABSTRACT

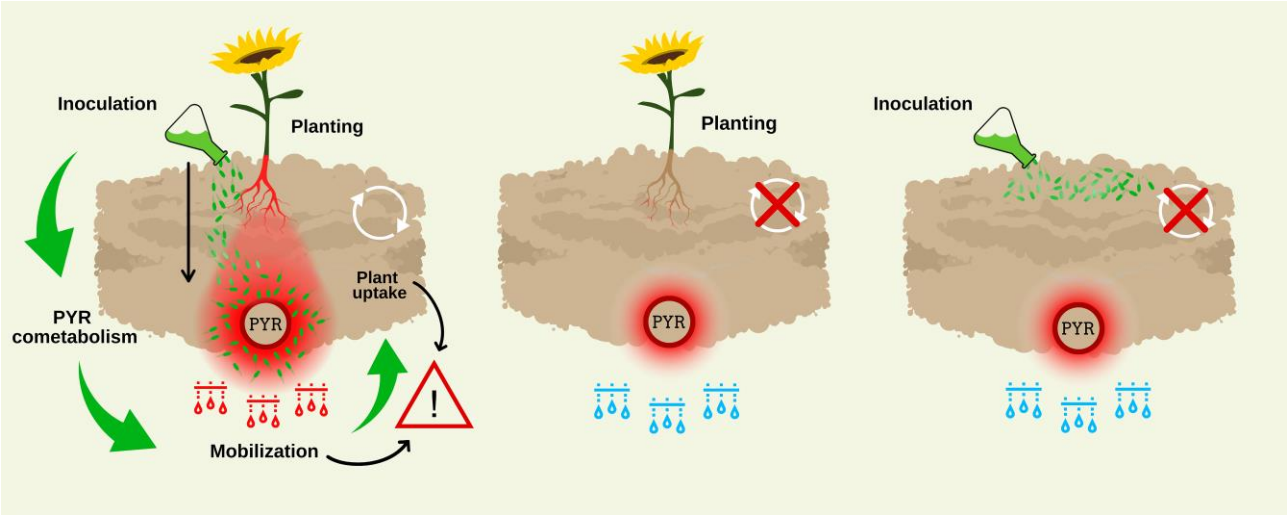

Introduction

The management of soil pollution by organic chemicals, such as polycyclic aromatic hydrocarbons (PAHs), through biological technologies evolved with the aim of remediating contamination on the basis of sustainable approaches. In this context, to enable realistic regulatory decisions, the fraction of pollutant present in soil that is available for uptake by organisms should be explicitly considered. Therefore, the bioavailability of pollutants in contaminated soils is an important area of scientific investigation. A pragmatic and justifiable approach for use in retrospective risk assessment was recently reported, which might be especially useful when decisions on soil remediation and reuse must be made [1]. Soil bioremediation can often initially increase chemical pollution risks as a result of biological processing of the most bioavailable pollutant fractions, leading to the formation of byproducts that are more toxic and mobile than the parent chemicals [1, 2] or to nonextractable residues with unknown risks [3]. In this context, and considering PAHs in particular, cometabolism is relevant; cometabolism is a major PAH removal mechanism and often results in incomplete transformation of the PAH molecular structure, leading to the formation of products that may have increased risks. This is substantially different from growth-linked microbial reactions, which are characterized by mineralization of PAHs, i.e., their complete conversion into harmless inorganic products. These potential sources of risks must be known to optimize the bioremediation of soils polluted by PAHs and other hydrophobic contaminants [4].

The flow of hydrophobic contaminants to degradative microbial communities in soil can be significantly affected by microbial positioning along the contaminant paths, which may result in enhanced or diminished biodegradation rates. These spatial factors may influence the contaminants associated with aggregates within the soil and those already being transported at macroscopic scales through the aqueous phase. The movement of contaminant-degrading microorganisms in porous media is usually limited by their high deposition rates and adhesion to soil surfaces. These

limitations can be overcome by flagellated microorganisms driven by behavioral responses to a variety of stimuli, including chemical gradients, leading to mobilization to distant contaminant sources and subsequently to an increased rate of contaminant uptake. The positive impact of such tactic bacterial mobilization on contaminant biodegradation was recently examined by our group in the model soil bacterium *Pseudomonas putida* G7 [5]. A variety of chemicals (including different sources of dissolved organic matter (DOM) and nanoparticles) caused different cellular motility patterns and enhanced bacterial transport, which increased the mineralization rate of naphthalene desorbed from a passive dosing device located a few centimeters away. In the absence of such stimuli, intrinsic flagellar motility led to limited bacterial transport and accessibility as a result of an enhanced tendency for deposition. This bacterium was also used as an experimental model for examining the potential role of bacterial motility in the cometabolism and biosorption of pyrene in a porous medium [6]. The study indicated that through these two processes, motile bacteria may even increase the risk associated with contaminant mobilization in soils.

The mechanism by which plants and their root-associated phenomena contribute to the mobilization of cometabolizing bacteria to distant pollutant sources in soil is unknown, and the concomitant risks caused by incomplete pollutant transformation due to cometabolism have yet to be identified. Some plant species appear to be more successful than others in stimulating the biodegradation of PAHs. Many studies have reported the aptitude of herbaceous species in remediating polluted soils with PAHs [4]. These beneficial functions in PAH biodegradation can be explained by both physical and physico-chemical processes that are involved in the relation between the plant root system and the soil microbiome in the rhizosphere, the soil zone in tight contact with roots [7, 8]. Among physical processes, soil aeration (drainage) of the pore space in soils is a fundamental factor affecting the mobility of bacteria, which can be transported passively (advected) by flowing streams of water or can move actively, primarily through flagellated motility or gliding [9]. Consequently, variations in soil hydration conditions due to drainage, water uptake by

plant roots and evaporation constantly alter microbial aqueous microhabitats [10], thus affecting microbial function and dispersal in soil [9]. On the other hand, root exudation by rhizodeposition releases root-derived C compounds (sugars, sugar alcohols, amino acids, and phenolics) that constitute substantial C and energy sources for bacteria and are targets of chemoreceptors; the consequent chemotaxis avoids many of the tortuous pathways associated with cell random walks [11, 12].

Sunflower (*Helianthus annuus* L.) connects food and energy and has a proven phytoremediation potential for soils polluted by PAHs [2, 11, 13]. This ability is due, on the one hand, to an extensive root system and strong positive geotropism allowing maximum colonization in a contaminated area, easing both passive and active transport by opening channels across the soil matrix. On the other hand, the high transpiration intensity at sunflower leaves regulates water flux in the soil and thus also contributes to phytoremediation [14]. In addition, we have reported the high tolerance of sunflower plants to PAHs [4, 14]. Therefore, according to our group experience [11, 15], sunflower, with its suitable radical system and high leaf evaporation level has been demonstrated to be adequate for the experimental purposes proposed.

To examine the relevance of cometabolic transformations of PAHs in the rhizosphere environment, the uptake and translocation of organic chemicals by the plant must be considered. These processes are a function of (a) the physicochemical properties of the target compounds, such as their hydrophobicity (represented by the octanol-water partitioning coefficient, log K_{ow}); (b) the environmental conditions, such as ambient temperature and the organic matter content of the soil; and (c) the plant species [16-18]. Hydrophobic molecules with a strong tendency to adsorb to soil may be less bioavailable than more hydrophilic compounds for plant uptake. The transfer and distribution of organic chemicals in soil-plant systems can be adequately described and interpreted by using partition and transfer coefficients [19]. In addition, bioconcentration factors (BCFs) and translocation factors (TFs) have been calculated by many authors to describe the range of chemical

uptake by plants; these factors are defined as the ratio of the chemical concentrations between plant biomass and soil solution and between plant biomass and root biomass, respectively [21-25, 20]. To the best of our knowledge, there are no other studies on the evolution of the whole sunflower ontogenetic cycle, that combine the use of a passive dosing system to control exposure of plant tissues to ^{14}C-labeled pollutants and BCF values from seed germination to fruit ripening.

In this study, we employed the bacterium *P. putida* G7 in a new model scenario to evaluate the potential role of sunflower plants in the accessibility and cometabolism of pyrene in soil. For this purpose, we employed a progressive approach by studying the cometabolic transformation of pyrene in soil slurries that contained silicone O-rings loaded with ^{14}C-pyrene, which acted as a passive dosing system. Then, under greenhouse conditions, we specifically tested whether cometabolically-active cells could access this source of sorbed pyrene when it was placed distant from the inoculation point in planted pots and facilitate uptake of the mobilized pollutant carbon by the roots.

2. Materials and methods

2.1 Chemicals

[4,5,9,10-^{14}C]-Pyrene (58.8 mCi mmol^{-1}, radiochemical purity >98%) was purchased from Campro Scientific GmbH (Veenendaal, The Netherlands), and ^{12}C-pyrene (purity 98%) was purchased from Sigma Aldrich (Madrid, Spain). Analytical-grade dichloromethane, acetonitrile, hexane and acetone were supplied by Fischer Chemical (Madrid, Spain). Silicone rings (O-rings) were obtained from Altec Products Ltd. (Cornwall, U.K.).

2.2 Soil

The soil used in this study was collected from the agricultural experimental station of the Instituto de Recursos Naturales y Agrobiología de Sevilla (IRNAS-CSIC). The soil was sieved (2 mm sieve)

before use. The physicochemical properties of the soil were as follows: pH 8.44; 0.44% total organic carbon (TOC); 0.75% organic matter; 0.046% organic nitrogen (Kjeldahl); 8.0 mg kg^{-1} Olsen phosphorus; and 122 mg kg^{-1} available potassium; the particle size distribution was 71.6% coarse-grained sand, 6.9% fine-grained sand, 10.6% silt, and 10.8% clay. The soil had a loamy-sandy texture. The concentration of native pyrene in this soil, determined as reported elsewhere [26], was 31.58 ± 9.55 μg kg^{-1}. This concentration corresponds to typical background concentrations of PAHs [27].

2.3 Cultivation of bacteria

The flagellated bacterium *P. putida G7*, which degrades pyrene by cometabolism, was cultivated and prepared differently for soil slurry experiments, metabolite analysis and greenhouse experiments. For soil slurry experiments, the strain was cultivated in 250-mL Erlenmeyer flasks with 100 mL of an inorganic salt solution (mineral medium (MM), pH 5.7) supplemented with 5 mM sodium salicylate as the sole carbon source and incubated at 30 °C on a rotary shaker at 150 rpm for 48 h, which was sufficient for reaching the early stationary phase and stable cell motility [6]. Cells were then centrifuged for 10 min at 9,087 *g* and resuspended in MM. The bacterial motility of the resuspended cells was confirmed by optical microscope observations. One milliliter of this suspension was used as inoculum for soil slurries to give a final cell density of 10^8 cell mL^{-1}. To extract and analyze pyrene metabolites, the bacterium was cultivated under the same conditions as described above but with an excess of pyrene (2.86 g L^{-1}) instead of salicylate as the sole carbon source, and the incubation period was extended to 7 days to reach a final optical density at 600 nm (OD_{600}) of 0.7.

In the greenhouse experiments, cultures were grown in two stages to obtain 4 L of culture for pot inoculation. In the first stage, 100 mL of bacterial culture produced as described for soil slurries was inoculated into two Erlenmeyer flasks (1 L) with 400 mL of MM supplemented with salicylate

and then cultivated as described above for 24 h. In the second stage, the cultures were divided into four 250-mL portions that were then transferred into individual 2-L flasks, diluted with 750 mL of MM with salicylate, and incubated for another 24 h to reach the early stationary phase (OD_{600} of 0.5 or 5×10^8 cell mL^{-1}) and therefore achieve stable cell motility, which was confirmed by microscopy of the final inocula. Cells were then harvested by centrifugation at 9,087 g for 10 min. The pellet was resuspended in 100 mL of MM without salicylate to give a cell density of 1.78×10^{10} cell mL^{-1}. Inoculation of each of the four pots with these suspensions (see section 2.7, Greenhouse experiment) resulted in a cell concentration of 4.45×10^{11} cell kg^{-1} soil.

2.4 Loading of O-rings with pyrene

A dynamic doping method was used to load the O-rings with ^{14}C-pyrene and ^{12}C-pyrene [5, 28]. In this study, O-rings of two different sizes were used. O-rings with an inner diameter of 50.47 mm and a cross section of 2.62 mm were used in the soil slurry experiments under laboratory conditions, whereas O-rings with an inner diameter of 145.72 mm and a cross section of 2.62 mm were used in the greenhouse experiments. In both cases, the loading procedure was the same, but the concentration of pyrene varied. Each ring was placed on the bottom of a 250-mL Erlenmeyer flask that contained 25 mL of an acetone solution containing ^{14}C-pyrene and unlabeled pyrene. The concentrations used were 125,135 dpm of ^{14}C-pyrene and 3.67 mg of unlabeled pyrene in the O-rings for the slurry experiments and 234,668 dpm of ^{14}C-pyrene and 23.75 mg of unlabeled pyrene in the O-rings for the greenhouse experiments. Some rings were loaded with the same amounts of unlabeled pyrene only. The flasks were left open overnight in a fume hood to allow complete evaporation of the acetone. To facilitate homogeneous incorporation of pyrene into the silicone, drops of Milli-Q water were then applied for two days. To confirm that the loading process was complete, individual rings were sacrificed and extracted for 96 h with 25 mL of methanol in screw-capped 250-mL Erlenmeyer flasks under continuous agitation (150 rpm). This extraction period was

sufficient for complete recovery of pyrene loaded into the rings, as revealed by preliminary extractions carried out over 60 days and involving successive substitutions with fresh methanol. The ^{14}C-pyrene present in the methanol extracts was quantified by liquid scintillation. One milliliter of the extracts was mixed with 5 mL of a liquid scintillation cocktail (Ultima Gold, Perkin Elmer, The Netherlands). The radioactivity was measured with a Beckman LS6500 liquid scintillation counter (Beckman Instruments, Fullerton, California, U.S.A.). The same methodology was followed to determine the amount of ^{14}C-pyrene remaining in the O-rings at the end of the greenhouse experiments.

2.5 Microbial transformation of pyrene in soil

In these assays, 250-mL Erlenmeyer flasks containing 30 g of soil, 69 mL of MM solution and a loaded silicone O-ring were inoculated with *P. putida* G7 cells, which were prepared as indicated above. The flasks were closed with Teflon-lined stoppers, from which a 5-mL vial containing 1 mL of 0.5 M NaOH was suspended to trap $^{14}CO_2$. The flasks were incubated at 23 ± 2 °C on an orbital shaker operating at 120 rpm. Control treatments lacked inoculum or soil. Each test was performed in duplicate.

Measurements of the mineralization of radiolabeled pyrene were carried out as described elsewhere [29]. To measure the partitioning of pyrene, the ^{14}C-labeled analyte concentrations were determined from the radioactivity in the aqueous suspension [6]. The concentrations were calculated from the initial amounts of labeled and unlabeled pyrene present in the O-rings and expressed as ^{14}C-pyrene equivalents partitioned into the aqueous phase to account for the likely transformation into pyrene byproducts through cometabolism. For this analysis, an aliquot from the suspension was centrifuged at 17,226 g for 10 min, and a fraction (1 mL) of the supernatant was mixed with 5 mL of liquid scintillation cocktail to measure radioactivity as described above. The rest of the aliquot was resuspended to its original volume with fresh MM and returned to the flask. Centrifugation was

not necessary and could therefore be avoided for the samples from the suspensions without soil because the bacterial biomass did not cause any interference due to quenching in the liquid scintillation measurements.

At the end of the assays, the flasks were sacrificed. The aqueous phase was separated from the soil by centrifugation, and the concentration of ^{14}C-pyrene equivalents in the supernatant was measured as described above. Soil samples were treated in an oxidizer (Model Sample Oxidizer, Perkin Elmer, combustion for 2 min with O_2) to determine residual ^{14}C by liquid scintillation. The O-ring from every flask was extracted with methanol, and the residual content of ^{14}C-pyrene was also measured by liquid scintillation. Unlabeled pyrene was also determined in soil samples from separate, duplicate flasks that were incubated under the same conditions but contained no ^{14}C-labeled compound, as previously described [27].

Radiorespirometry measurements in solid-phase conditions were performed in Erlenmeyer flasks as described above for the soil slurry experiments, with 60 g of soil, where the O-ring was buried. The soil received no inoculum. The humidity was adjusted with 19 mL of distilled water to reach a value similar to that in the greenhouse experiment.

2.6 Extraction and analysis of pyrene metabolites

To extract and analyze pyrene metabolites, a 20-mL sample from a *P. putida G7* culture prepared as above (section 2.3) was centrifuged at 17,226 g for 10 min, and the supernatant was extracted five times with equal volumes of ethyl acetate. This new extract was concentrated with a rotary evaporator, and its volume was further reduced under a nitrogen flow to 1 mL. The pyrene degradation products present in this solution were identified by full-scan gas chromatography - mass spectrometry (GC-MS). The full-scan GC-MS analyses were performed on a Thermo Scientific TSQ8000 equipped with a ZB-5MS capillary column. The method used was similar to a previously described method [30]. The flow rate of the carrier gas was 1 mL min^{-1}. The mass spectra

of individual total ion peaks were identified by comparison with spectra in a mass spectral database (NIST MS Search 2.0).

Derivatization was carried out to increase the volatility and thermal stability of the compounds during GC analysis [30]. The method used was similar to a previously described method [6]. Briefly, silylation was achieved by evaporating the samples and then introducing trimethylsilyl (TMS) groups using N,O-bis-trimethylsilyl acetamide, pyridine and trimethylchlorosilane (final volume 150 µL). The reaction was achieved by vortexing the samples and leaving them in the dark for 1 h. The full-scan GC-MS analyses of the derivatized samples were performed on a Thermo Scientific TSQ8000 equipped with a ZB-1MS capillary column with a specific GC temperature program. The flow rate of the carrier gas was 1 mL min^{-1}. The mass spectra of individual total ion peaks were identified by comparison with spectra in a mass spectral database (NIST MS Search 2.0).

2.7 Variations in the numbers of *Pseudomonas putida* G7 cells in soil slurries, simulated rhizosphere soil and soil leachates over time

To test the time evolution of the viable cell numbers of *P. putida* G7, two experiments were designed with soil slurries and soil percolation columns. The cell densities of the inocula were the same as those applied in the soil slurry experiment for testing the cometabolism of fully accessible pyrene and in the greenhouse experiment. In both conditions, the influence of the rhizosphere was simulated by the addition of sunflower root exudates, which were previously obtained from sunflower plants propagated in vitro [12]. The exudate solution had 459 mg total organic carbon (TOC) L^{-1} and caused a positive tactic response (tactic factor of 47.8) in *P. putida* G7, determined with capillary assays [12]. Every slurry and column experiment was performed in duplicate.

For the soil slurries, the experiments were performed under the same conditions as above (section 2.5), with the difference that in this case the slurries did not contain pyrene-loaded O-rings,

and that the inoculated cells were added to the slurries after resuspension in the root exudates. At certain time intervals, 1 mL samples were collected from each flask, inoculated on TSA agar plates after appropriate dilutions in MM, and incubated for 48 h at 30 ºC, to determine the number of colony-forming units (CFUs) of *P. putida* G7. The soil percolation column experiment was carried out in 140-mL funnels equipped with 40 mm-pore glass frits (5.6 cm diameter), where the soil was packed to reach a length of 7 cm, to mimic the depth at which the O-ring was introduced into the pots in the greenhouse experiment. The inoculation procedure and the adjustment of soil water content was also the same as described for the greenhouse experiment, but adapted to the amount of soil (250 g dry soil). The root exudates (24 mL with 337 mg TOC L^{-1}) were added to the columns right after inoculation. At certain time intervals, distilled water was added to the top of the columns and the leachates were collected by gravity immediately after irrigation. The number of *P. putida* G7 CFUs was determined in the leachates as described above for the soil slurries. The columns were sacrificed after 24 h, and soil samples were extracted with a hand auger. The samples were then divided into two equal portions (upper and lower parts). A portion (5.5 g wet weight) of each of these subsamples was mixed with MM and dispersed to form a slurry. Then, the number of *P. putida* G7 CFUs was determined as described above. The total cell recovery in this column experiment was 99.7 ± 15.9 % in the control and 104.5 % ± 12.2 in the rhizosphere-simulated soil.

2.8 Greenhouse experiment

2.8.1 Experimental design

The experiment was carried out in a greenhouse at 23 ± 1 °C using a total of 12 pots. The pots were 18.5 cm high, and the maximum and minimum diameters were 21.5 and 15.0 cm, respectively. A hole at the bottom of each pot allowed the collection of leachates during the experiment. Each pot received 4 kg of soil, which reached a height of 14 cm upon packing. The pots were classified into two different groups: those that received an O-ring loaded with ^{12}C- and ^{14}C-pyrene (6 labeled pots, numbers 1 to 6) and those loaded with only ^{12}C-pyrene (6 unlabeled pots, numbers 7 to 12). The

unlabeled pots were used to estimate soil dehydrogenase (DH) activity. In each group, there were three different treatments, each one performed in duplicate: planted inoculated pots (pots 1, 2, 7 and 8), planted noninoculated pots (3, 4, 9 and 10) and unplanted inoculated pots (5, 6, 11 and 12). The O-rings were introduced into the pots at 7 cm from the upper soil surface during soil packing.

The soil water content in each pot that did not receive a bacterial inoculum was adjusted to 100% water-holding capacity with 1.3 L of sterile distilled water. In inoculated pots, the water content was adjusted stepwise to minimize osmotic shock to the inoculated bacteria. Initially, the water-holding capacity was 50%, and sterile distilled water was used. After approximately 6 h, 100 mL of an MM suspension (described in section 2.3) of *P. putida* G7 cells was added to each pot. After approximately 3 h, the rest of the distilled water was added to achieve 100% of the water-holding capacity. The water content of every pot was adjusted to 100% water-holding capacity every 3-4 days until harvest. Two additional inoculations with *P. putida G7* were performed at 20 and 64 days following the same methodology as the first inoculation, with the only difference being that no additional water was added. These two inoculation time points were selected on the basis of 1) the lag phase for pyrene mineralization observed in laboratory incubations of noninoculated soil and 2) the evolution of plant growth under these greenhouse conditions.

The sunflower seed coats were removed, and the naked seeds were stored at 9 °C until cultivation. Twenty of these naked seeds were used per planted pot. Throughout the sunflower development cycle, the percentage of seed germination and the blooming evolution and stem length of plants were separately evaluated for each treatment. Although each treatment studied in the greenhouse experiment was performed in duplicate, the results are expressed separately for every replicate.

2.8.2 Sample collection

Samples of leachates, soil and plants were taken at different sampling time points. Leachate sampling was performed to determine the ^{14}C- activity at the start, at 1.5 days, and then 2 days a week for the first month of sowing. Later, leachate samples were collected 1 day per week until the end of the experimental period. Leachates were collected by gravity immediately after each irrigation event. Samples of soils and plants were collected at days 36, 57, 78 and 106 after sowing. The soil samples were extracted with a hand auger from each pot. These samples were then divided into two subsamples, one corresponding to the first 7 cm of depth and a second representing the next 7 to 14 cm, to study the effect of the O-ring that had been placed in the middle of every pot. Both soil and leachate samples were stored at -80 °C until analysis to prevent microbial activity. The sampling points in the pots were different each time, and the resulting holes were refilled afterwards with a similar volume of fresh soil to avoid creating preferential paths for water drainage. At the same sampling time, one plant per pot was carefully pulled out to avoid root damage. The plant was washed with distilled water, and leaves, stems, roots and fruits (when present) were stored separately at -80 °C until further use. At the end of the experimental period, the O-rings were collected from the pots to determine the residual radioactivity. In the planted pots, the O-ring was colonized by the plant roots.

A control was run for the third inoculation of the pots (at 64 days) by determining the number of colony-forming units (CFUs) of *P. putida G7* in leachate samples from planted and unplanted inoculated pots up to 6 days after inoculation. A portion of the leached liquid from the pots without ^{14}C was collected, inoculated on TSA agar plates, and incubated for 48 h at 30 °C. The numbers of CFUs were determined to establish possible bacterial percolation through irrigation. The results indicate that the recovery of bacteria in the leachates was maximal after 24 h and was higher in the planted pots (245.5 ± 14.5 CFU L^{-1} and 120.0 ± 21.9 CFU L^{-1} in planted and unplanted pots, respectively). However, given the high cell density of the inoculum, these low recoveries indicate that most of the added bacteria were retained in the pots, independent of the presence of the plants.

350

351 **2.8.3 Extraction and analysis of pyrene**

352 To measure the concentration of ^{14}C-pyrene equivalents in the leachates, an aliquot (10 mL) was
353 mixed with 10 mL of liquid scintillation cocktail (Ultima Gold XR, PerkinElmer). Radioactivity
354 was measured by liquid scintillation in a Beckman counter as described above. To determine ^{14}C in
355 soil and sunflower plant samples, 1 g of sample was placed into a combustion cone, which was then
356 combusted in an oxidizer (previously described in section 2.5). The samples obtained after
357 combustion were measured in the same way as the leachates, but in this case, the results are
358 expressed as ^{14}C activity per weight of dry material. Only the results with plant samples are
359 reported because the ^{14}C activity detected in soil samples was very low (maximum value 9 dpm g^{-1})
360 and did not differ significantly between the different treatments in the two soil layers analyzed
361 (above and below the O-rings). At the end of the greenhouse experiment, the O-rings from every pot
362 were also extracted, and the concentration of ^{14}C-pyrene was measured as described above.

363

364 **2.8.4 Calculation of the bioconcentration and fruit translocation factors**

365 In this study, we assumed that the radioactivity determined in plant samples corresponded to ^{14}C-
366 pyrene. We hypothesized that any significant differences between treatments in the plant uptake or
367 transfer rates of this hydrophobic chemical were indications of plant uptake of polar metabolites
368 generated by the modified bacterial accessibility and cometabolism of this PAH in soil. Therefore,
369 the BCF for ^{14}C-pyrene was calculated using the following previously reported equation [20] with
370 some modifications:

371 $$BCF\ (L\ kg^{-1}) = \frac{\mathrm{Cp}\frac{dpm\ kg^{-1}\,\mathrm{dry\ weight}}{\mathrm{N}}}{\mathrm{Cs}\ (dpm\ L^{-1})} \qquad (1)$$

372 where C_p is the ^{14}C activity per kilogram of dry belowground (roots) or aboveground (stems, leaves
373 and fruits) plant biomass, N is the number of plants in each pot at the specific time of sampling, and
374 C_s is the ^{14}C activity per liter of soil solution. In this equation, the C_p values were normalized to the

actual number of plants to account for the possible influences of the different individual plants in each pot on pyrene mobilization and uptake. The values of C_s were calculated assuming constant partitioning of ^{14}C-pyrene from the O-ring, serving as a reservoir, into the aqueous medium:

$$Cs = \frac{\Sigma(Cf - C0)}{\Sigma(Vi - Vl)} \quad (2)$$

where C_f is the ^{14}C activity (dpm) in the O-ring measured at the end of the experiment, C_o is the ^{14}C activity (dpm) in the O-ring measured at the start of the experiment, V_i is the volume of irrigation water (mL), and V_l is the volume of leachate (mL). The final percentage of the initial ^{14}C activity present in the O-rings at the end of the experiment, determined after methanol extraction, was 19.31 ± 3.9% for planted inoculated pots and 20.91 ± 0.8% for planted noninoculated pots. This result indicates that the two treatments behaved similarly under comparable conditions in terms of *in situ* passive dosing.

Mature fruits were observed and collected only at the end of the greenhouse experiment. The fruit TF (FTF) was calculated to evaluate the transfer of ^{14}C activity from roots to fruits. The FTF was calculated as the ratio between the ^{14}C activity in fruits and that in roots, assuming that the contribution of the fruits to pyrene mobilization and uptake was negligible:

$$FTF = \frac{Cfr}{Cr/N} \quad (3)$$

where *Cfr* is the ^{14}C activity per g of dry fruit biomass, *Cr* is the ^{14}C activity per g of dry root biomass, and *N* is the number of plants in each pot at the time of sampling.

2.8.5 Estimation of soil dehydrogenase activity

The DH activity of the soil in the pots was determined by the reduction of the tetrazolium salt iodonitrotetrazolium chloride (INT) to yield iodonitrotetrazolium formazan (INTF) as described elsewhere [31, 32]. Briefly, 1 g of soil was weighed in glass tubes. To this sample, 0.2 mL of a 0.4% INT solution and 0.6 mL of distilled water were added. To the controls, only 0.8 mL of water was added. The tubes were capped and incubated for 20 h at 25 °C in the dark. The reaction was stopped

400 by the addition of 10 mL of methanol. The samples were filtered, and the absorbance at 490 nm was
401 measured. Every soil sample was measured in triplicate. The concentration of INTF was calculated
402 from a calibration curve. To calculate the enzymatic activity, the absorbance of the controls was
403 subtracted from that of the samples, and the activity is expressed as μg INTF g^{-1} dry soil h^{-1}. For the
404 calculation, a soil sample was oven-dried at 80 °C for 48 h to establish the soil dry weight.
405
406 **3. Results**
407 **3.1 Bacterial accessibility and cometabolism of pyrene in soil slurries**
408 The soil slurry experiment made it possible to evaluate the bacterial transformation of pyrene by *P.*
409 *putida* G7 in soil, which would later be tested under greenhouse conditions. Batch incubations were
410 performed in inoculated slurries with ^{14}C-labeled pyrene loaded in silicone O-rings. The evolution
411 of the concentration of ^{14}C-pyrene equivalents in the aqueous phase over time is shown in Figure
412 1A. The results indicate that, both with and without soil, the bacterium caused the concentration of
413 ^{14}C-labeled pyrene equivalents to quickly reach values well above the aqueous solubility of pyrene.
414 During the same experimental period (approximately the first week), no mineralization was
415 observed (Figure 1B). This lack of mineralization indicates that the phenomenon detected was a
416 cometabolic reaction producing water-soluble metabolites; this reaction has already been studied
417 with this strain in liquid suspensions and sand percolation columns [6]. In the absence of soil, the
418 aqueous concentration of pyrene equivalents reached an approximate value of 10 mg L^{-1} after one
419 week, which remained somewhat constant until the end of the experiment. This concentration
420 indicates that approximately 20% of the pyrene mass initially loaded in the O-ring partitioned into
421 the aqueous phase as a result of cometabolism. The lower but sustained concentration in the soil
422 slurries (approximately 2 mg L^{-1}) than in the bacterial suspensions without soil could be attributed
423 to the sorption of pyrene metabolites to soil particles. Indeed, the analysis of residual ^{14}C recovered
424 through an oxidizer from the soil at the end of the experiment showed that the concentration of ^{14}C-

425 labeled pyrene equivalents was 11.68 ± 2.77 mg kg^{-1}. This value is several orders of magnitude
426 higher than the pyrene concentration of 65.32 ± 21.96 μg kg^{-1} measured by HPLC in soil from
427 slurries maintained under the same conditions without ^{14}C, which is consistent with the presence of
428 pyrene metabolites adsorbed to the soil.

429 Pyrene mineralization occurred in the soil slurries but did not occur in the absence of soil
430 (Figure 1B). Therefore, the bacterial strain used in this study did not mineralize this compound [6];
431 the autochthonous microbial population was likely responsible, though with a long (30 days)
432 acclimation phase. To confirm this supposition, a mineralization control was run with noninoculated
433 soil, both under slurry conditions and in the solid phase (Figure S1B and S1C, respectively). The
434 phase of maximum mineralization occurred later under solid-phase conditions (approximately after
435 45 days), but the rates were very similar to those in noninoculated slurries (Table S1). The evolution
436 of the concentration of ^{14}C-labeled pyrene equivalents in these slurries (Figure S1A) over the entire
437 experimental period evidenced the presence of water-soluble pyrene transformation products,
438 although at significantly lower concentrations (i.e., 0.95 mg L^{-1} after 7 days) than those in the
439 slurries that had received the *P. putida* G7 inoculum. These results are consistent with the
440 background concentration of native pyrene detected in the soil, indicating previous exposure of the
441 autochthonous microbial population to this chemical. Such exposure would have led to the
442 development of pyrene biodegradation capability in the soil [27]. Given the long acclimation phase
443 needed for pyrene mineralization and that the slurry experiment was designed to test the fast
444 cometabolism of pyrene by the added *P. putida* G7 cells under conditions facilitating full access to the
445 pollutant source, we did not consider it necessary to characterize the microbial populations that were
446 already present in the soil.
447

448 **3.2. Identification of pyrene metabolites**

Extraction and identification of pyrene metabolites was performed as indicated in section 2.6. The extracts were studied with and without derivatization. The extracts without derivatization showed the presence of only one metabolite, 1-hydroxypyrene. The spectrum of this metabolite (molecular mass of 218 and retention time (t_R) of 31.20 min) had a significant fragment ion at *m*/*z* 189 corresponding to the fragmentation pattern of 1-hydroxypyrene, which matched data in the mass spectral library. The same metabolite was found previously in a study in our laboratory on the cometabolism of pyrene [6], but in the current case, we extended the study to other metabolites by culturing the bacterium in an excess of solid substrate. The derivatized extracts were analyzed, and two additional metabolites were identified: phthalic acid and benzoic acid. In this analysis, the fragment ion at m/z 73 (characteristic of silylation) was selected, and the mass spectra of the obtained silylated derivatives are shown in Figure 2. A peak with a molecular mass of 290, a t_R of 11.92 min, significant fragment ions at m/z 189, 215, 244, 259, and 275 (corresponding to a fragmentation pattern), and a match in the mass spectral library was attributed to a silylated derivative of 1-hydroxypyrene (Figure 2A). Another peak, with a molecular mass of 310, a t_R of 9.56 min, a significant fragment ion at m/z 295 (corresponding to a fragmentation pattern), and a match in the mass spectral library, was attributed to a silylated derivative of phthalic acid (Figure 2B). Another peak, with a molecular mass of 282, a t_R of 9.32 min, significant fragment ions at m/z 193, 223, and 267 (corresponding to a fragmentation pattern), and a match in the mass spectral library, was identified as a silylated derivative of benzoic acid (Figure 2C). Pyrene peaks were identified in all chromatograms, indicating that pyrene was not completely degraded by *P. putida* after one week of incubation under these conditions. The GC chromatograms are shown in Figure S2, with main peaks corresponding to the retention times for 1-hydroxypyrene and the silylated derivative of 1-hydroxypyrene (31.59 and 11.92 min, respectively).

3.3 Variations in the numbers of *Pseudomonas putida* G7 cells in soil slurries, simulated rhizosphere soil and soil leachates over time

The soil slurry experiment (Figure 3A) showed that, in the absence of exudates, *P. putida* G7 was still viable after 7 days (the period during which the cometabolism of pyrene was observed in the soil slurries- Figure 1A), both in the soil slurry and in the control with MM only. However, during that period, the number of viable cells decreased in the soil slurry by up to three orders of magnitude with respect to the initial number (from $4.6 \pm 0.2 \times 10^8$ CFU mL^{-1} to $3.0 \pm 0.1 \times 10^5$ CFU mL^{-1}) and was significantly lower than the number of viable cells in the soil-free control at that time ($1.4 \pm 0.1 \times 10^8$ CFU mL^{-1}). The presence of exudates did not extend the viability of the bacterium in the soil slurries, as evidenced by the similar number of *P. putida* G7 cells that survived after 7 days ($2.2 \pm 0.4 \times 10^5$ CFU mL^{-1}) compared with the results of soil slurries without exudates.

The soil percolation column results evidenced significantly higher numbers of cells in the leachates of columns that had received the exudates (Figure 3B). The enhancement of transport was evident during the first 16 h, after which the number of cells mobilized by exudates was double to that in the control without exudates ($13.7 \pm 0.7 \times 10^8$ CFU vs. $7.2 \pm 0.2 \times 10^8$ CFU, accounting for, respectively, 13.1 % and 6.9 % of the total number of cells introduced into the soil). After 24 h, the columns were sacrificed, and the number of cells that remained in the soils was determined separately in the upper and lower parts of each column. A higher number of cells was found in the upper parts of the control columns without exudates than in their lower parts ($2.6 \pm 0.4 \times 10^7$ CFU g^{-1} and $1.2 \pm 0.2 \times 10^7$ CFU g^1, respectively). Very similar bacterial numbers were found at both levels of the columns that had received the exudates ($1.8 \pm 0.3 \times 10^7$ CFU g^{-1} and $1.9 \pm 0.1 \times 10^7$ CFU g^{-1}, respectively, in the upper and lower parts). These results demonstrate an enhanced bacterial transport through soil in the presence of exudates.

3.4 Greenhouse experiment

3.4.1 Plant response

The maximum seed germination rate was 30.6%, which occurred 21 days after the start of the greenhouse experiment. As the experiment progressed, the plant length reached averages of 33.3 cm and 63.1 cm after 36 and 78 days, respectively, with maximum lengths of 46 cm and 74 cm on these sampling days. Variations in the number of germinated seeds in each pot resulted in different initial numbers of plants per pot, and during the experiment, sampling of individual plants was performed (Figure 4A and 4B, Table S2). To minimize alteration of the packed soil structure as a result of the plant extraction, which would eventually result in preferential flow paths for the irrigated water (and, eventually, the inocula), the number of individuals per pot was not standardized by additional extractions. The flowering period started at 72 days, with 3.3% of the plants flowering, and 90.3% of the plants were flowering at day 85. In accordance with the ontogenetic cycle of sunflower in the assayed greenhouse conditions, the plants started to decline at day 89. No significant differences between the studied parameters in relation to bacterial inoculation were found (Student's t-test $p \leq 0.05$).

3.4.2 Mobilization of ^{14}C-pyrene into leachates and plants

3.4.2. A) Concentration of ^{14}C-pyrene equivalents in leachates

The time evolution of the concentration of ^{14}C-pyrene equivalents in the leachates and the number of plants per pot are presented in Figure 4. Inoculations were performed at the three stages indicated by the arrows in the figure: at the start, after 20 days, and after 64 days. The initial inoculation and plant development had no effect on the leachates during the initial phase (20 days). However, a sharp increase in the concentration of ^{14}C-pyrene equivalents was observed 7 days after the second inoculation (Figure 4A). This increase was not observed without inoculation in planted pots or in inoculated, unplanted pots (Figure 4B and 4C, respectively). The different numbers of plants in each

planted and inoculated pot correlated well with the differences observed between the two plots regarding the enhanced concentrations of ^{14}C-pyrene equivalents. Indeed, the specific amount of pyrene mobilized per plant in these leachate samples was similar in both pots. The average value, 8.75 ± 1.91 µg plant^{-1}, was significantly different (Student's t-test $p \leq 0.05$) from that of the same leachate sample from noninoculated planted pots (1.05 ± 0.07 µg plant^{-1}). The third inoculation also caused root-mediated pyrene mobilization, but mobilization was delayed to 16 days and occurred only in the pot with the highest number of plants. However, the intensity of this enhancement (9.72 µg plant^{-1}) in this pot similar to that observed for the first inoculation (10.10 µg plant^{-1}).

3.4.2. B) Bioconcentration and fruit translocation factors

The BCF values in belowground and aboveground plant samples at different times after sowing are shown separately for each pot in Table 1. In all the treatments, the ^{14}C activity in the belowground plant samples was generally higher than that in the aboveground plant samples. The maximum root BCF values were found on day 36 in pots 1, 3 and 4, whereas pot 2 showed its highest value at day 57. The delay observed in this pot was probably related to the lower number of plants that had developed (Figure 4A). Assuming that the number of plants in the pot had a role in pyrene mobilization and uptake (similar to the above calculations with leachates), the concentration of ^{14}C-pyrene equivalents in the root material exhibiting the maximum BCF value in each pot was normalized to the total number of plants present at the time of sampling (as indicated in Figure 4). This calculation yielded significantly different (Student's t-test $p \leq 0.05$) values: 13.53 ± 0.37 µg g^{-1} and 6.32 ± 0.93 µg g^{-1} for the inoculated (pot 1 at 36 days, pot 2 at 57 days) and noninoculated (pots 3 and 4 at 36 days) treatments, respectively. This result indicates that the enhanced concentrations of ^{14}C-pyrene equivalents detected in the leachates 7 days after the second inoculation translated into a doubled specific plant uptake rate, independent of the number of plants.

This enhanced root uptake caused by the bacterial inoculations did not clearly affect the aboveground BCF values (Table 1). However, the FTF values calculated from the radioactivity measured in the fruits at the end of the experimental period were significantly different. Planted inoculated pots showed fruit ^{14}C activity values of 57 and 137 dpm g^{-1} (pots 1 and 2, respectively), while noninoculated pots showed fruit ^{14}C activity values of 65 and 40 dpm g^{-1} (pots 3 and 4, respectively). The resulting FTF ratios, normalized for the number of plants present in each pot, were 2.19 ± 0.03 in the inoculated pots and 3.95 ± 0.07 in the noninoculated pots. Therefore, inoculation caused a decrease (Student's t-test, $p \leq 0.05$) in the root-to-fruit transfer of ^{14}C-labeled equivalents.

3.4.3 Estimation of soil dehydrogenase activity

Before the beginning of the experiment, DH activity was measured in the soil used for the experiments. That activity was considered the basal activity on day 0 for all the treatments. The presence of sunflower plants had a major influence on DH activity, as shown in Figure 5. Thus, planted pots, independent of whether they were inoculated, showed significantly higher DH activity than treated unplanted pots. This difference occurred both in the top 7 cm of the soil and in the bottom of the pots. The increase in DH activity was significantly lower when no plants were present and was observed only in the upper part of the pot. At the bottom of the pot, the DH activity was not different from the basal activity found on 0, even after the two additional inoculations at days 20 and 62 (Figure 5).

4. Discussion

In this study, we analyzed the effect of sunflower plants on the bacterial accessibility and cometabolism of pyrene located at a spatially distant source within the soil. For this analysis, we compared the transformation of ^{14}C-labeled pyrene in experiments with batch slurries and planted

572 pots that were inoculated with *P. putida* G7. This bacterium combines flagellar cell motility with the
573 ability to cometabolically transform PAHs, two microbial traits recently identified as contributors to
574 risks associated with pollutant mobilization during bioremediation [6]. Furthermore, the bacterium
575 reacts chemotactically to DOM components released *in vitro* by sunflower plants, which results in
576 enhanced transport through water-saturated sand [12] and enhanced mineralization of distantly located
577 (cm away) naphthalene in sand columns [5]. Our results extend these previous findings by showing
578 that (i) the inoculated bacterium accessed the distant pyrene source only after the plants had
579 developed in the soil and that (ii) the resulting cometabolic transformation of pyrene caused
580 mobilization of the metabolites to the plant roots.

581 The enhanced concentration of ^{14}C-pyrene equivalents detected in the leachates of planted
582 pots after the second and third bacterial inoculations (Figure 4A) indicates that the plants facilitated
583 locomotion of the inoculated bacterium to the vicinity of the O-rings. The first inoculation,
584 performed at the start of the experiment, had no effect on leachate concentrations because previous
585 plant development was necessary for mobilization. No enhancement was observed in planted pots
586 that were not inoculated. This result excludes any direct influence of sorption to biochemical DOM
587 components, produced by sunflower plants [11, 33] on the mobilization of pyrene. The absence of
588 mobilization in unplanted inoculated pots can be explained by the significant deposition of bacterial
589 cells in the upper zones of the soil, therefore preventing access to and cometabolism of pyrene. This
590 limited dispersal of the bacterial inoculum into deeper soil zones is consistent with the low DH
591 activity detected in the bottom of these pots (Figure 5 C2). Although we did not directly measure
592 the deposition of bacteria in the exposure zone close to the O-rings, the results from the transport
593 experiment with and without root exudates, performed with column lengths comparable to the depth
594 at which the O-rings were located in the pots, are also consistent with bacterial mobilization caused
595 by planting towards the distant pollutant source. Furthermore, the enhanced concentrations
596 measured in the effluent of planted inoculated pots (approximately 1 mg L^{-1}, Figure 4A) were on

597 the same order as those measured in inoculated soil slurries (Figure 1A), where the bacteria had full
598 access to the pollutant source. This concentration exceeds the water solubility of pyrene (0.135 mg
599 L^{-1}) by ten times, which indicates the presence of metabolites more hydrophilic than pyrene. Indeed,
600 the three metabolites identified in *P. putida* G7 pyrene- cometabolizing cultures, 1-hydroxypyrene,
601 benzoic acid and phthalic acid, have lower log K_{ow} values (4.6, 1.87 and 0.73, respectively) than
602 pyrene (4.88) [34, 35]. In accordance with their molecular structure and the metabolic pathways
603 proposed elsewhere for pyrene biodegradation [30, 36, 37], these metabolites would have still contained
604 the radiolabeled C originally present in the ^{14}C-labeled pyrene molecules, which would have
605 permitted their detection by liquid scintillation.

606 Given the fortuitous nature of the cometabolic transformation of high-molecular weight
607 (HMW) PAHs, leading to the formation of products that do not enter into the bacterial central
608 metabolism, the rates of these transformations in soil are typically slow [4]. The inoculation of soil
609 with a high number of cometabolically competent cells performed in this study was part of our
610 model scenario but may constitute a valid alternative to enhance the rates of cometabolic
611 degradation, especially for HMW PAHs that are only biodegraded through cometabolism (for
612 example, benzo(a)pyrene). Under these conditions, the cometabolism of the target chemical would
613 be dominated by the related PAH-degrading genes from the inoculated strain. Because the focus of
614 our study was the influence of sunflower plants on bacterial accessibility to pyrene located at a
615 spatially distant source within the soil, we did not attempt a genetic and biochemical study of
616 pyrene cometabolism in the target bacterial strain, *P. putida* G7. Given the interest in combining
617 cell motility with PAH cometabolism, these types of studies should be the subject of future
618 research. However, in our study, the identification of three common metabolites previously
619 identified in known pyrene biodegradation pathways suggests that metabolic cooperation with other
620 bacteria that are able to accommodate these metabolites in their central metabolism (leading to
621 mineralization) is possible. Indeed, such cooperation could be a possible explanation for the

622 mineralization observed in the soil slurry experiment, where after a long acclimation phase, the
623 autochthonous microorganisms might have been able to mineralize the metabolites produced by the
624 cometabolic action of *P. putida* G7 on pyrene.

625 These results are consistent with the essential functions played by plant roots in soil
626 exploration, acquisition of minerals and water uptake [7]. In our experimental conditions, where the
627 soil was saturated with water for an extended period of time, the motile character of *P. putida* G7
628 may have favored root-mediated dispersion of cells through planted soil. Indeed, the transport of
629 this bacterium is enhanced through chemotaxis to sunflower DOM components, which tends to
630 reduce cell deposition in porous environments due to modified cell motility behavior (Jimenez-
631 Sanchez et al., 2015, 2018). However, it is also possible that the root network provided physical
632 pathways for dispersal of this chemotactic bacterium in soil, analogous to the effect caused by
633 mycelial pathways in soil, along which this and other flagellated bacteria can be dispersed through
634 their own chemotactic navigation [38]. The enhancement observed in our study was not likely caused
635 by a metabolic need for an alternate carbon source (such as root components) on the cometabolism
636 of pyrene by this strain, as the bacterium readily cometabolized the compound in the absence of any
637 other carbon source (Figure 1A). The results for the evolution of viable cell numbers in soil slurries
638 (Figure 3A) suggest that root exudation did not extend the survival of *P. putida* G7 cells in bulk
639 soil. However, an effect of roots by providing suitable niches for the colonization and survival of *P.*
640 *putida* G7 in the vicinity of the O-rings, cannot be excluded, and it should be the subject of future
641 research.

642 The higher root BCF values in inoculated pots than in pots without inoculation indicate that
643 the ^{14}C-labeled transformation products from cometabolism detected in soil leachates also settled, at
644 least partially, in the plant biomass. This enhanced ^{14}C-activity accumulated in the roots, and hence,
645 its concentration in the aboveground plant samples was relatively low throughout the experiment
646 (Table 1). Generally, the uptake of nonpolar compounds by plant roots occurs through passive

647 diffusive partitioning and is positively correlated with water transpiration. Furthermore, the more
648 hydrophilic a compound is, the more easily it accumulates in roots and is translocated from the base
649 to the apex of the plants, while most lipophilic organic compounds may strongly partition into the
650 epidermis of the roots and not be transferred into the inner root zones, becoming translocated within
651 the plant [24]. Furthermore, within plants, chemicals can undergo a variety of enzymatic reactions and
652 be converted into insoluble or even irreversibly bound products [19]. Indeed, inoculation increased the
653 plant uptake rate of ^{14}C-pyrene equivalents but decreased the relative transfer of ^{14}C-pyrene
654 equivalents to the roots, as evidenced by lower FTF ratios. Therefore, the different BCF and FTF
655 values in planted pots with and without inoculation could reflect different plant behaviors with
656 respect to the metabolites produced by *P. putida* G7, those produced by the microbial soil
657 populations, and the parent compound. These results can be explained by postulating that the
658 metabolites produced by *P. putida* G7 have a high affinity for root tissues and that metabolite
659 transformation products formed in the roots, which would have reduced the migration of mobilized
660 ^{14}C to the rest of the plant body.

661 The potential of the autochthonous soil populations to transform pyrene, as detected in the
662 laboratory incubations, may raise questions related to the extent to which this process occurred
663 under greenhouse conditions and how such transformation would have contributed to the plant
664 biomass ^{14}C contents and the BCF and FTF values. Because our focus was on determining pyrene
665 accessibility and cometabolism, we used highly dense bacterial inocula of *P. putida* G7, which
666 readily cometabolized pyrene. Therefore, the inoculation activity with respect to pyrene likely
667 overwhelmed that of the autochthonous soil microorganisms. However, our results do not rule out
668 the biodegradation of pyrene or even its mineralization in the soils of the noninoculated pots, which
669 would eventually have led to uptake of transformation products by the plants. Previous studies
670 about the fate of CO_2 transported internally by plants from belowground [39, 40] have reported that the
671 concentration of xylem sap CO_2 is limited under nonstressed physiological conditions, such as those

672 operating here, and mainly depends on the respiratory activity of the root system involved.
673 Consequently, the $^{14}CO_2$ absorbed by roots and eventually released into the soil solution in the
674 noninoculated pots can be considered irrelevant, which points to the uptake of pyrene and microbial
675 metabolites by plants grown in thesepots.

676 In addition to providing evidence for a root-mediated enhancement of microbial accessibility
677 and cometabolism in soil, this study provides, to our knowledge, the first evidence of plant uptake
678 of the metabolites produced by microbial cometabolism of PAHs. Possibly as a result of the unique
679 experimental design employed, which involved passive dosing under greenhouse conditions and the
680 growth of sunflower plants to the completion of their ontogenetic cycle with cometabolic
681 transformation of a coexisting pollutant, the BCF values reported here differ from those inother
682 studies on the bioaccumulation of pyrene and PAHs in general by plants. In many plant species,
683 belowground and aboveground BCF values for pyrene have been calculated or reported for different
684 exposure media (air, soil, water and sediment) and different plant growth conditions, and
685 consequently, the reported units vary as well. For example, the belowground BCF values for pyrene
686 ranged between 168 L kg^{-1}-dw (dry weight) and 1,272 L kg^{-1}-dw in Longijing tea plants [22], whereas
687 the reported BCF values for PAHs were 512 L kg^{-1}-ww (wet weight) for wheat roots [23], 67 L kg^{-1}-
688 dw and 0.46 L kg^{-1}-dw for belowground and aboveground ryegrass biomass [41] and 39-1349 L kg^{-1}-
689 ww and 2.1-10.4 L kg^{-1}-ww for belowground and aboveground red clover, respectively [25]. All the
690 above studies were conducted using either batch techniques with seedlings that were hydroponically
691 cultured and exposed to known amounts of solid PAHs or directly with field-contaminated soils,
692 which are very different experimental conditions from those used here. In our greenhouse
693 experiment, the reproducible conditions provided by passive dosing reliably controlled the exposure
694 of the inoculated bacterium and plants in the soil environment to pyrene. Therefore, our study
695 extends the range of application of passive dosing techniques, which have been successfully used in

696 a variety of aquatic and sediment toxicity tests, such as in determining toxicity to soil invertebrates
697 [42-44].

698 Our study highlights that the biological processing of PAHs in soil may cause problems under
699 certain circumstances. A solution to these problems can be provided by future research on risk-
700 based modulation of these pollutant carbon fluxes through bioavailability approaches. For example,
701 future innovations may involve the comobilization of immotile (i.e., nonflagellated) bacterial strains
702 able to mineralize metabolites, thus expanding the catabolic potential of the microbial inocula. The
703 promotion of root processes leading to the formation of nonbioavailable (and therefore nontoxic)
704 pollutant residues in root tissues, through optimization of the plant physiology and the use of other
705 plant species could also be part of future investigations.
706

707 **4.1. Conclusions**

708 In this study, we experimentally integrated passive dosing with ^{14}C-labeled pyrene, inoculation of
709 motile bacteria into soil and a complete sunflower ontogenetic cycle to examine a new scenario
710 related to pollutant transformation and risk in soil. We demonstrated that sunflower plants can
711 facilitate access of a representative soil bacterium with combined cell motility and cometabolic
712 actions on pyrene in soil located at a distant source. Moreover, the resulting metabolites were not
713 only mobilized into the soil leachates but also taken up by the plants, accumulating in the roots at
714 significantly higher proportions in inoculated samples than in uninoculated controls and behaving
715 differently on their way to the fruits. This new, proof-of-concept scenario successfully showed that
716 bacterial cometabolism may contribute to the environmental risk from PAHs in soil by enhancing
717 pollutant mobilization and uptake by plants. These results are relevant in the bioremediation field
718 because they show how inoculated bacteria can be mobilized by plants to reach distant pollutant
719 sources and how partial pollutant transformation may generate further issues. Our results may also

720 contribute to other pollution management sectors, such as wastewater treatment and prospective risk
721 evaluation of agrochemicals, where rhizosphere microorganisms play a relevant role.
722

723 ## 5. Acknowledgments

724

725 We thank the Spanish Ministries of Economy and Competitiveness (CGL2016-77497-R) and
726 Science and Innovation (PID2019-109700RB-C21) for supporting this work.
727

728 **References**

729

730 1. Ortega-Calvo, J. J.; Harmsen, J.; Parsons, J. R.; T.Semple, K.; Aitken, M. D.; Ajao, C.;
731 Eadsforth, C.; Galay-Burgos, M.; Nidu, R.; Oliver, R.; Peijnemburg, W. J. G. M.; Römbke, J.;
732 Streck, G.; Versonnen, B., From Bioavailability Science to Regulation of Organic Chemicals.
733 *Environmental Science and Technology* **2015,** *49,* 10255-10264.
734

735 2. Sivaram, A. K.; Logeshwaran, P.; Lockington, R.; Naidu, R.; Megharaj, M., Impact of plant
736 photosystems in the remediation of benzo[a]pyrene and pyrene spiked soils. *Chemosphere* **2018,**
737 *193,* 625-634.
738

739 3. Harmsen, J., Hennecke, D., Hund-Rinke, K., Lahr, J., Deneer, J., Certainties and uncertainties
740 in accessing toxicity of non-extractable residues (NER) in soil. *Environmental Sciences Europe*
741 **2019,** *31,* 99.
742

743 4. Ortega-Calvo, J. J.; Tejada-Agredano, M. C.; Jimenez-Sanchez, C.; Congiu, E., Sungthong,
744 R.; Niqui-Arroyo, J. L.; Cantos, M., Is it possible to increase bioavailability but not environmental

745 risk of PAHs in bioremediation?. *Jounal of Hazardous Materials* **2013,** *261,* 733-745.
746
747 5. Jimenez-Sanchez, C., Wick, L.Y., Ortega-Calvo, J.J., Impact of Chemoffectors on Bacterial
748 Motility, Transport, and Contaminant Degradation in Sand-Filled Percolation Columns.
749 *Environmental Science and Technology* **2018,** *52* 10673-10679.
750
751 6. Rolando, L.; Vila, J.; Posada-Baquero, R.; Castilla-Alcantara, J. C.; Barra Caracciolo, A.;
752 Ortega Calvo, J. J., Impact of bacterial motility on biosorption and cometabolism of pyrene in a
753 porous medium. *Science of The Total Environment* **2020,** *717,* 137210.
754
755 7. Ortiz-Castro, R., Lopez-Bucio, J., Review: Phytostimulation and root architectural responses
756 to quorum-sensing signals and related molecules from rhizobacteria. *Plant Science* **2019,** *284,* 135-
757 142.
758
759 8. Bourceret, A.; Leyval, C.; Thomas, F.; Cébron, A., Rhizosphere effect is stronger than PAH
760 concentration on shaping spatial bacterial assemblages along centimetre-scale depth gradients.
761 *Canadian Journal of Microbiology* **2017,** *63,* 881-893.
762
763 9. Ebrahimi, A. N.; Or, D., Microbial dispersal in unsaturated porous media: Characteristics of
764 motile bacterial cell motions in unsaturated angular pore networks. *Water Resources Research* **2014,**
765 *50,* (9), 7406-7429.
766
767 10. Wang, G.; Or, D., A hydration-based biophysical index for the onset of soil microbial
768 coexistence. *Scientific Reports* **2012,** *2,* 881.
769

770 11. Tejeda-Agredano, M. C.; Gallego, S.; Vila, J.; Grifoll, M.; Ortega-Calvo, J. J.; Cantos, M.,
771 Influence of sunflower rhizosphere on the biodegradation of PAHs in soil. *Soil Biology and*
772 *Biochemistry* **2013,** *57,* 830-840.
773
774 12. Jimenez-Sanchez, C.; Wick, L. Y.; Cantos, M.; Ortega-Calvo, J. J., Impact of dissolved
775 organic matter on bacterial tactic motility, attachment, and transport. *Environmental Science and*
776 *Technology* **2015,** *49,* 4498-4505.
777
778 13. Liduino, V. S.; Servulo, E. E. C.; Oliveira, F. J. S., Biosurfactant-assisted phytoremediation of
779 multi-contaminated industrial soil using sunflower (*Helianthus annuus L.*). *Journal of*
780 *Environmental Science and Health* **2018,** *Part A, 53,* (7), 609-616.
781
782 14. Ortega-Calvo, J. J., Posada-Baquero, R., García, J. L., Cantos, M. , Bioavailability of
783 polycyclic aromatic hydrocarbons in soil as affected by microorganisms and plants. In *Soil*
784 *biological communities and ecosystem resilience*, Lukac, M., Grenni, P. and Gamboni, M., Ed.
785 Springer: 2017; pp 305-319.
786
787 15. Sungthong, R.; van West, P.; Cantos, M.; Ortega-Calvo, J. J., Development of eukaryotic
788 zoospores within polycyclic aromatic hydrocarbon (PAH)-polluted environments: A set of behaviors
789 that are relevant for bioremediation. *Science of The Total Environment* **2015,** *511,* 767-776.
790
791 16. Dettenmaier, E. M.; Doucette, W. J.; Bugbee, B., Chemical hydrophobicity and uptake by
792 plant roots. *Environmental Science and Technology* **2009,** *43,* 324-329.
793
794 17. Su, Y.; Liang, Y., Foliar uptake and translocation of formaldehyde with Bracket plants

795 *(Chlorophytum comosum)*. *Jounal of Hazardous Materials* **2015,** *291,* 120-128.
796
797 18. Trapp, S., Bioaccumulation of polar and ionizable compounds in plants. In *Ecotoxicology*
798 *Modeling*, Devillers, J., Ed. Springer: Dordrecht (The Netherlands), 2009; pp 299-353.
799
800 19. Trapp, S.; Matthies, M.; Scheunert, I.; Topp, E. M., Modeling the bioconcentration of organic
801 chemicals in plants. *Environmental Science and Technology* **1990,** *24,* 1246-1252.
802
803 20. González García, M.; Fernández-López, C.; F., P.; S., T., Predicting the uptake of emerging
804 organic contaminants in vegetables irrigated with treated wastewater – Implications for food safety
805 assessment. *Environmental Research* **2019,** *172,* 175-181.
806
807 21. Yang, Z.; Zhu, L., Performance of the partition-limited model on predicting ryegrass uptake of
808 polycyclic aromatic hydrocarbons. *Chemosphere* **2007,** *67,* 402-409.
809
810 22. Daohui, L.; Lizhong, Z.; Wei, H.; Jouying, T., Tea Plant Uptake and Translocation of
811 Polycyclic Aromatic Hydrocarbons from Water and around Air. *Journal of Agricultural and food*
812 *chemistry* **2006,** *54,* 3658-3662.
813
814 23. Tao, Y.; Zhang, S.; Wang, Z.; Christie, P., Predicting Bioavailability of PAHs in Soils to
815 Wheat Roots with Triolein-Embedded Cellulose Acetate Membranes and Comparison with
816 Chemical Extraction. *Jounal of Agricultural and Food Chemistry* **2008,** *56,* 10817-10823.
817
818 24. Doucette, W. J.; Shunthirasingham, C.; Dettenmaier, E. M.; Zaleski, R. T.; Fantke, P.; Arnotf,
819 J. A., A Review of Measured Bioaccumulation Data on Terrestrial Plants for Organic Chemicals:

820 Metrics, Variability, and the Need for Standardized Measurement Protocols. *Environmental*
821 *Toxicology and Chemistry* **2018,** *37,* 21-33.
822
823 25. Gao, Y.; Shen, Q.; Ling, W.; Ren, L., Uptake of polycyclic aromatic hydrocarbons by
824 *Trifolium pretense* L. from water in the presence of a nonionic surfactant. *Chemosphere* **2008,** *72,*
825 636-643.
826
827 26. Posada-Baquero, R.; López-Martín, M.; Ortega-Calvo, J. J., Implementing standardized
828 desorption extraction into bioavailability-oriented bioremediation of PAH-polluted soils. *Science of*
829 *The Total Environment* **2019,** *696,* 134011.
830
831 27. Posada-Baquero, R.; Ortega-Calvo, J. J., Recalcitrance of polycyclic aromatic hydrocarbons
832 in soil contributes to background pollution. *Environmental Pollution* **2011,** *159,* 3692-3699.
833
834 28. Smith, K. E. C., Rein, A., Trapp, S., Mayer, P., Karlson, U. G. , Dynamic passive dosing for
835 studying the biotransformation of hydrophobic organic chemicals: microbial degradation as an
836 example. *Environmental Science and Technology* **2012,** *46,* 4852-4860.
837
838 29. Posada-Baquero, R.; Niqui-Arroyo, J. L.; Bueno-Montes, M.; Gutierrez-Daban, A.; Ortega
839 Calvo, J. J., Dual ^{14}C/residue analysis method to assess the microbial accessibility of native
840 phenanthrene in environmental samples. *Environmental Geochemistry and Health* **2008,** *30,* 159-
841 163.
842
843 30. Hadibarata, T.; Kristanti, R. A., Biodegradation and metabolite transformation of pyrene by
844 basidiomycetes fungal isolate *Armillaria sp. F022*. *Bioprocess and Biosystems Engineering* **2013,**

845 *36*, 461-468.

846

847 31. Trevors, J. T., Dehydrogenase-activity in soil - A comparison between the int and ttc assay.
848 *Soil Biology and Biochemistry* **1984,** *16* 673-674.

849

850 32. García, C.; Hernández, T.; Costa, F.; Ceccanti, B.; Masciandaro, G., In the dehydrogenase
851 activity of soil as an ecological marker in processes of perturbed system regeneration. In
852 *Proceedings of the XI International Symposium of Environmental Biogeochemistry.*, Gallardo-
853 Lancho, J., Ed. Salamanca (Spain), 1993; pp 89-100.

854

855 33. Posada-Baquero, R.; Nienke Jiménez-Volkerink, S.; Garcia, J.-L.; Cantos, M.; Grifoll, M.;
856 Ortega-Calvo, J. J., Rhizosphere-enhanced biosurfactant action on slowly desorbing PAHs in
857 contaminated soil. *Science of The Total Environment* **2020,** *720:13*.

858

859 34. Hansch, C.; Leo, A.; Hoekman, D., Exploring QSAR: Hydrophobic, Electronic, and Steric
860 Constants. *American Chemical Society: Washington, DC.* **1995**.

861

862 35. PubChem, Database. 1-hydroxypyrene, CID=21387,
863 https://pubchem.ncbi.nlm.nih.gov/compound/21387#section=Computed-Properties. *National*
864 *Center for Biotechnology Information* **2020**.

865

866 36. Haritash, A. K.; Kaushik, C. P., Biodegradation aspects of Polycyclic Aromatic Hydrocarbons
867 (PAHs): A review. *Journal of Hazardous Materials* **2009,** *169*, 1-15.

868

869 37. Cochran, R. E.; Dongari, N.; Jeong, H.; Beránek, J.; Haddadi, S.; Shipp, J.; Kubátová, A.,

870 Determination of polycyclic aromatic hydrocarbons and their oxy-, nitro-, and hydroxy-oxidation
871 products. *Analytica Chimica Acta* **2012,** *740,* 93-103.
872
873 38. Furuno, S.; Päzolt, K.; Rabe, C.; Neu, T. R.; Harms, H.; Wick, L. Y., Fungal mycelia allow
874 chemotactic dispersal of polycyclic aromatic hydrocarbon-degrading bacteria in water-unsaturated
875 systems. *Environmental Mycrobiology* **2010,** *12,* 1391-1398.
876
877 39. Teskey, R. O.; McGuire, M. A., CO_2 transported in xylem sap affects CO_2 efflux from
878 *Liquidambar styraciflua* and *Platanus occidentalis* stems, and contributes to observed wound
879 respiration phenomena. *Trees-Structure and Function* **2005,** *19*, 357-362.
880
881 40. Zach, A.; Horna, V.; Leuschner, C., Diverging temperature response of tree stem CO_2 release
882 under dry and wet season conditions in a tropical montane moist forest. *Trees-Structure and*
883 *Function* **2010,** *24*, 285-296.
884
885 41. Yang, Z., Zhu, L., Performance of the partition-limited model on predicting ryegrass uptake of
886 polycyclic aromatic hydrocarbons. *Chemosphere* **2007,** *67,* 402-409.
887
888 42. Mayer, P.; Holmstrup, M., Passive dosing of soil invertebrates with polycyclic aromatic
889 hydrocarbons: Limited chemical activity explains toxicity cutoff. *Environmental Science and*
890 *Technology* **2008,** *42,* 7516-7521.
891
892 43. Bandow, N.; Altenburger, R.; Lubcke-von Varel, U.; Paschke, A.; Streck, G.; Brack, W.,
893 Partitioning-based dosing: An approach to include bioavailability in the effect-directed analysis of
894 contaminated sediment samples. *Environmental Science and Technology* **2009,** *43,* 3891-3896.

44. Smith, K. E. C.; Dom, N.; Blust, R.; Mayer, P., Controlling and maintaining exposure of hydrophobic organic compounds in aquatic toxicity tests by passive dosing. *Aquatic Toxicology* **2010,** *98,* 15-24.

Figure legends

Figure 1. Evolution over time of the concentration of ^{14}C-pyrene equivalents in the aqueous phase (A, including an expanded insert with the same axis labels at the top right of this figure) and mineralization of ^{14}C-pyrene (B) in inoculated soil slurries inoculated with *Pseudomonas putida* G7 (■) and an inoculated control without soil (▲). The maximum rates and extents of mineralization measured in these tests are summarized in Table S1. Error bars represent one standard deviation.

Figure 2. Mass spectra of the silylated derivatives of metabolites identified as 1-hydroxypyrene (A), phthalic acid (B) and benzoic acid (C) in pyrene-cometabolizing cultures of *Pseudomonas putida* G7. The molecular structure assigned to each derivative is shown in each figure.

Figure 3. Evolution over time of the number of *Pseudomonas putida* G7 cells (as colony forming units, CFUs) in soil slurries (A) and in the leachates of soil percolation columns (B) with and without sunflower root exudates. The treatments in A had mineral medium only (▲), soil slurries without exudates (■, solid line), and soil slurries with exudates (■, dotted line). In B, the total number of cells present in the leachates with (dotted bars) and without (black bars) exudates is presented. When visible, error bars indicate one standard deviation.

Figure 4. Evolution of the concentration of ^{14}C-pyrene equivalents in leachate samples (black) in planted inoculated pots (A), planted noninoculated pots (B) and unplanted inoculated pots (C). The number of plants per pot (gray) is also shown (panels A and B). In each panel, the results for each duplicate pot are represented individually with different symbols for pots 1, 3 and 5 (■), and for pots 2, 4 and 6 (●). The arrows indicate inoculations with *Pseudomonas putida* G7.

Figure 5. Soil DH activity in planted inoculated pots (A), planted noninoculated pots (B) and unplanted inoculated pots (C) at two different depths: 0-7 (A1 to C1) and 7-14 (A2 to C2) cm. In each panel, the results for each duplicate pot are represented individually with different symbols for pots 7, 9 and 11 (■), and for pots 8, 10 and 12 (●). The arrows indicate inoculations with *Pseudomonas putida* G7.

Figure 1.

925

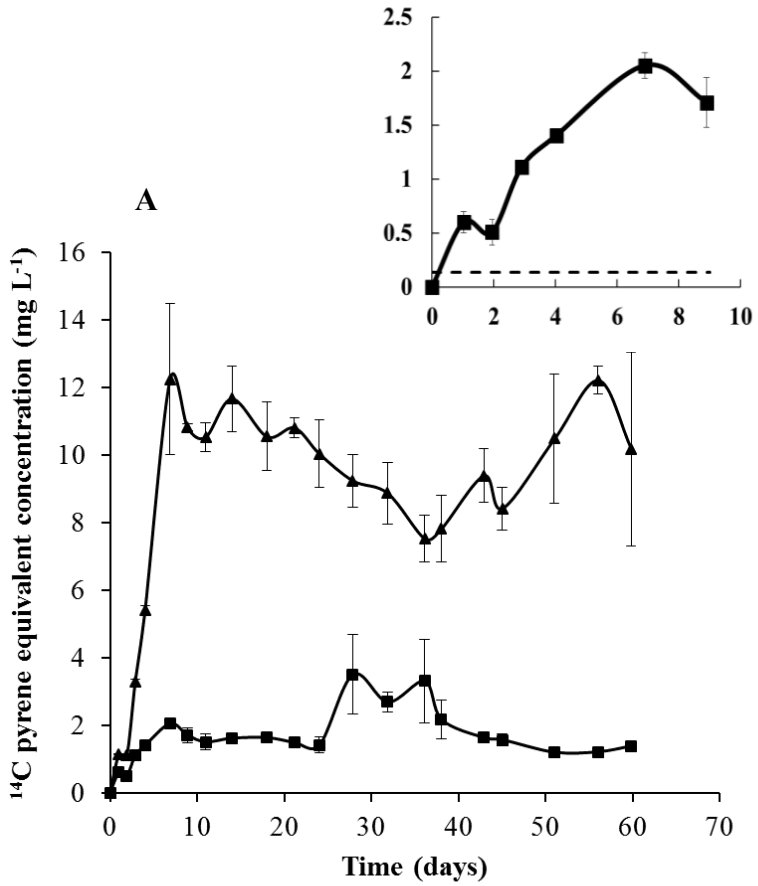
A
^{14}C pyrene equivalent concentration (mg L^{-1})
Time (days)
0
2
4
6
8
10
12
14
16
0
10
20
30
40
50
60
70
0.5
1
1.5
2
2.5

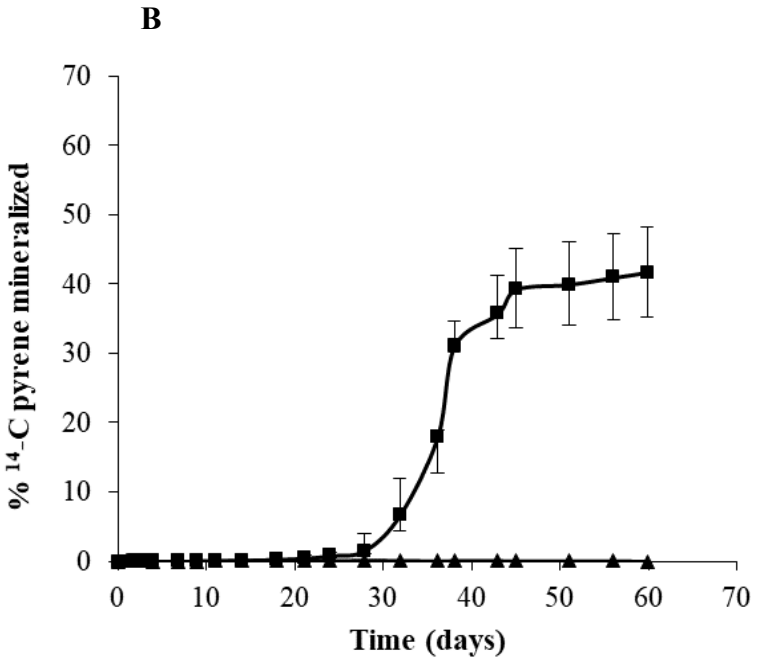
B
% ^{14}-C pyrene mineralized
Time (days)
0
10
20
30
40
50
60
70

926 **Figure 2**

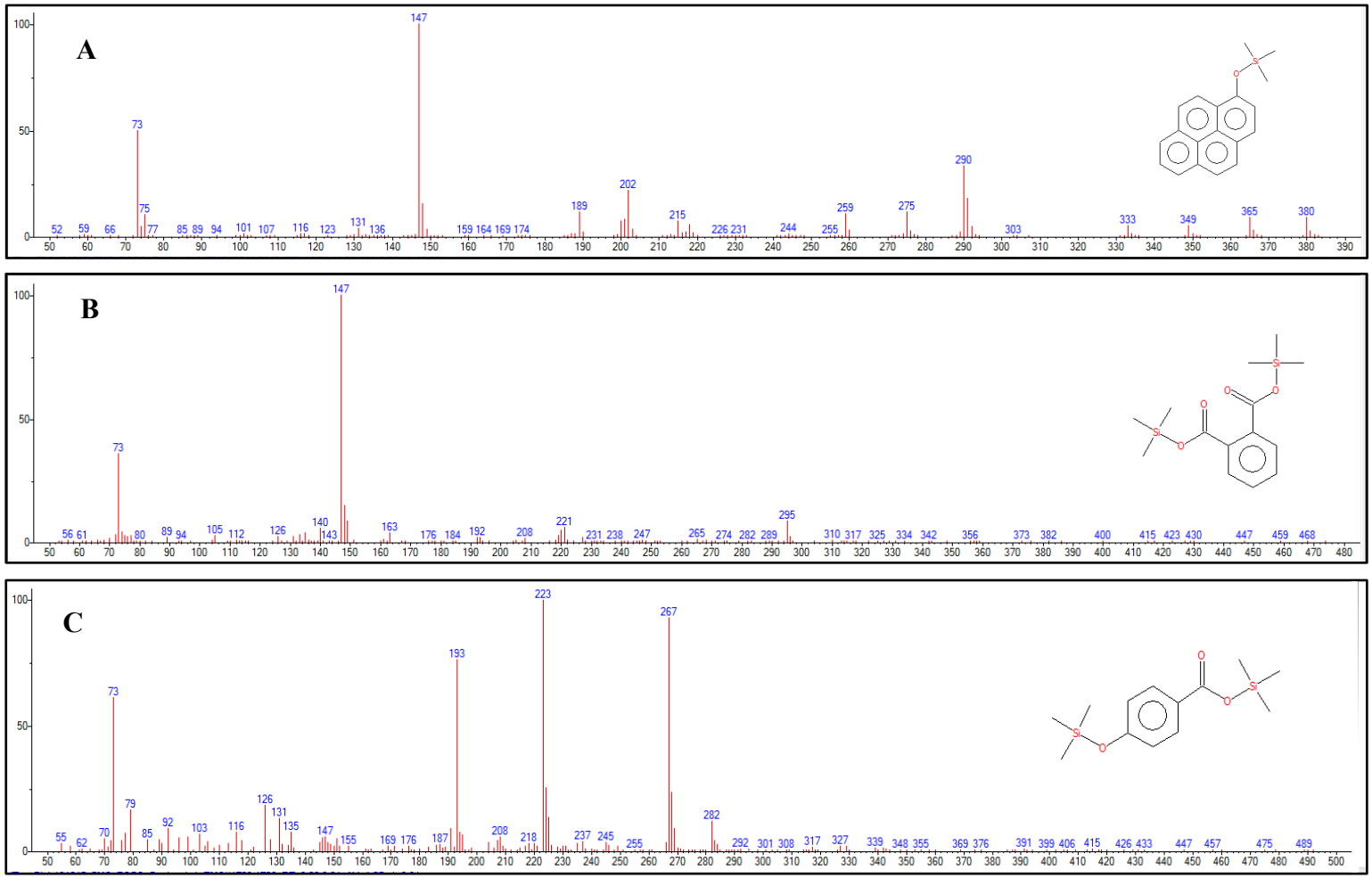

Figure 3

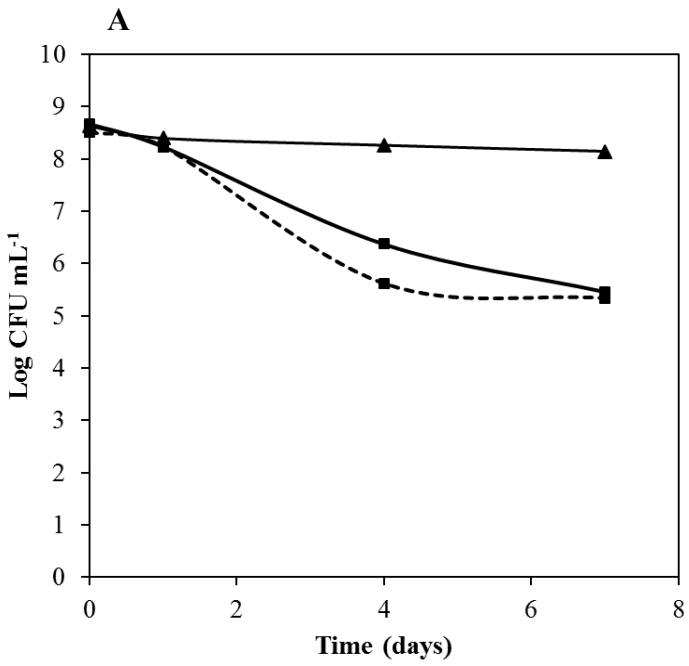

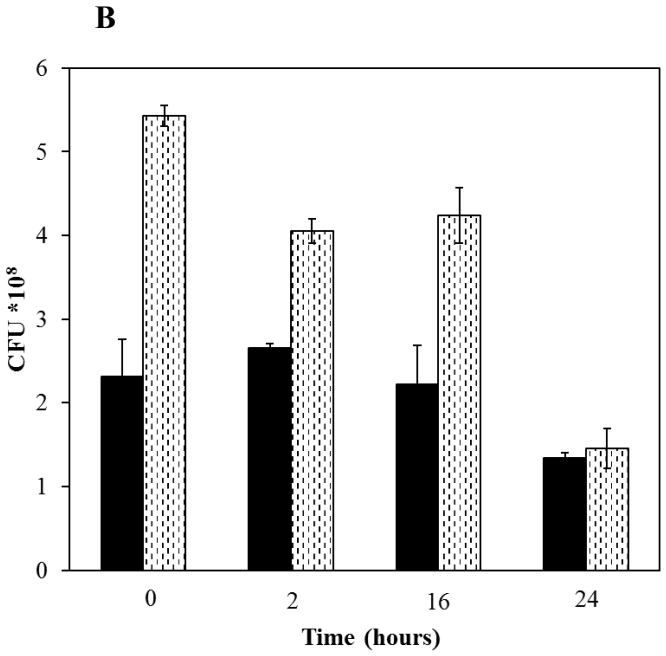

Figure 4

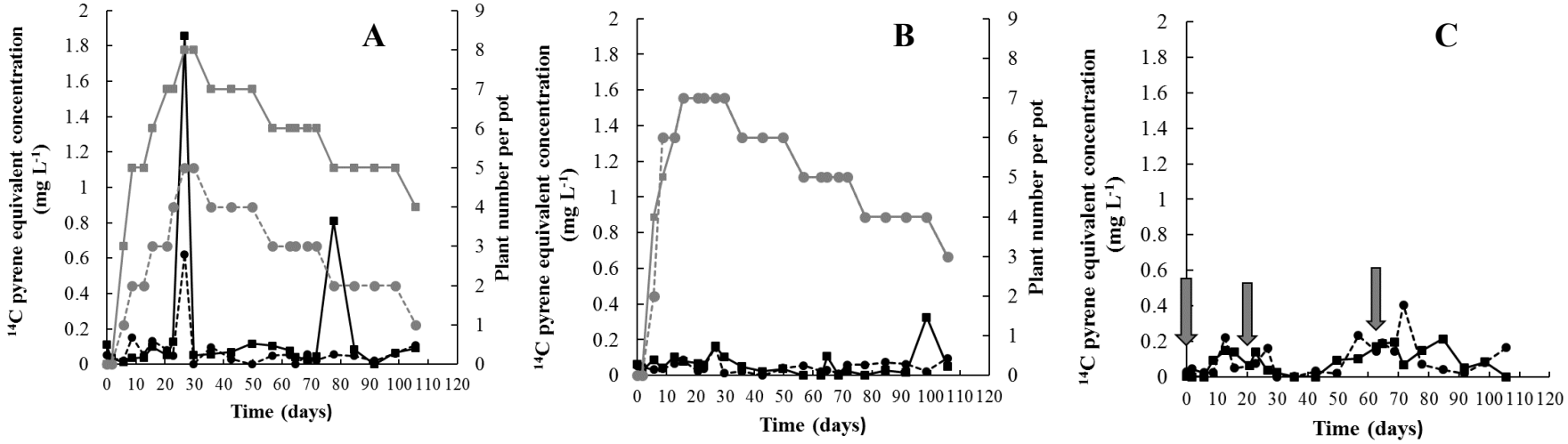
A
B
C
^{14}C pyrene equivalent concentration (mg L^{-1})
Plant number per pot
Time (days)
0 10 20 30 40 50 60 70 80 90 100 110 120
0 0.2 0.4 0.6 0.8 1 1.2 1.4 1.6 1.8 2
0 1 2 3 4 5 6 7 8 9

Figure 5

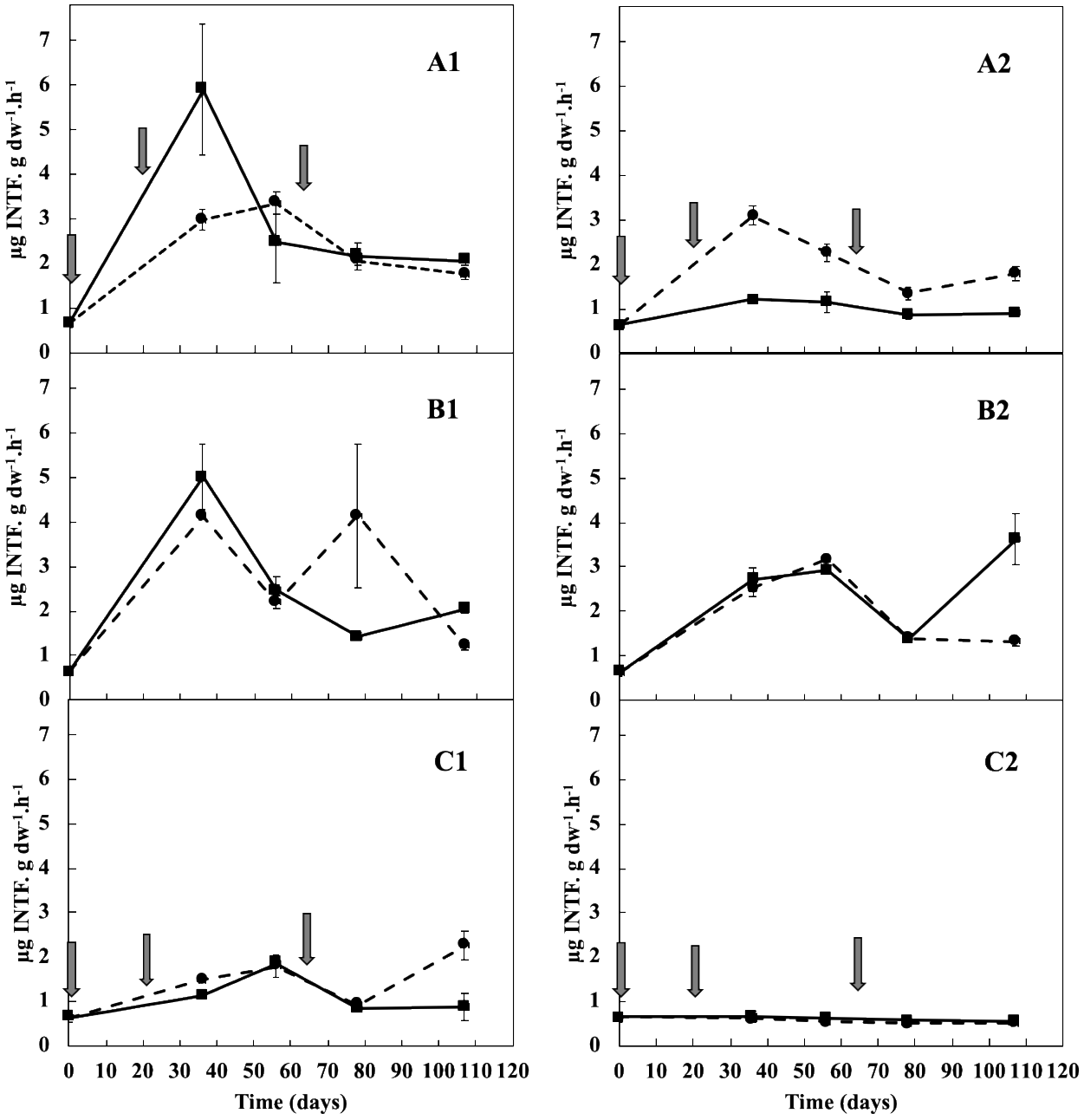
A1
A2
B1
B2
C1
C2
µg INTF. g dw-1.h-1
Time (days)
0 10 20 30 40 50 60 70 80 90 100 110 120
0 1 2 3 4 5 6 7

Table 1. Bioconcentration factors (L kg^{-1}) in belowground (roots) and aboveground (stems, leaves and fruit) plant samples under greenhouse conditions.

	Belowground				Aboveground			
Day	POT 1[a]	POT 2[b]	POT 3[c]	POT 4[d]	POT 1	POT 2	POT 3	POT 4
36	0.43 (929)	0.07 (86)	0.24 (419)	0.19 (340)	0.03 (68)	0.02 (34)	0.03 (58)	0.05 (96)
57	0.05 (160)	0.25 (414)	0.04 (95)	nd[e]	0.03 (105)	0.04 (97)	0.02 (66)	0.02 (63)
78	0.01 (53)	0.07 (217)	0.08 (430)	0.02 (124)	0.01 (47)	0.03 (101)	0.02 (87)	0.02 (119)
106	0.01 (103)	0.02 (63)	0.01 (65)	0.01 (41)	0.01 (75)	0.07 (189)	0.02 (151)	0.01 (67)

[a,b] Duplicate pots of treatment soil with both bacteria and sunflower plants, [c,d] duplicate pots of treatment soil with sunflower plants. The values in parentheses indicate the radioactivity in the plant tissue samples (dpm g^{-1} dry weight) [e]Value below background.